

Molecular motors transporting cargos in viscoelastic  
cytosol:  
how to beat subdiffusion with a power stroke?

Igor Goychuk<sup>1</sup>,  
Vasyl O. Kharchenko  
Institute of Applied Physics  
Natl. Acad. Sci. Ukraine, Sumy, Ukraine,

Ralf Metzler  
Institute for Physics and Astronomy,  
University of Potsdam, Karl-Liebknecht-Str. 24/25,  
14476 Potsdam-Golm, Germany  
& Department of Physics, Tampere University of Technology,  
Korkeakoulunkatu 3, 33101 Tampere, Finland

<sup>1</sup>Corresponding author. Address: Institute for Physics and Astronomy, University of Potsdam, Karl-Liebknecht-Str. 24/25, 14476 Potsdam-Golm, Germany, e-mail: igoychuk@uni-potsdam.de, Tel.: (049)331-977 5614, Fax: (049)331-977-1045

## Abstract

Anomalous slow passive diffusion,  $\langle \delta x^2(t) \rangle \simeq t^\alpha$ , with  $0 < \alpha < 1$ , of larger tracers such as messenger RNA and endogenous submicron granules in the cytoplasm of living biological cells has been demonstrated in a number of experiments and has been attributed to the viscoelastic physical nature of the cellular cytoplasm. This finding provokes the question to which extent active intracellular transport is affected by this viscoelastic environment: does the subdiffusion of free submicron cargo such as vesicles and organelles always imply anomalously slow transport by molecular motors such as kinesins, that is, directed transport characterized by a sublinear growth of the mean distance,  $\langle x(t) \rangle \simeq t^{\alpha_{\text{eff}}}$ , with  $0 < \alpha_{\text{eff}} < 1$ ? Here we study a generic model approach combining the commonly accepted two-state Brownian ratchet model of kinesin motors based on the continuous-state diffusion along microtubule driven by a flashing binding potential. The motor is elastically coupled to a cargo particle, which in turn is subject to the viscoelastic cytoplasmic environment. Depending on the physical parameters of cargo size, loading force, amplitude of the binding potential, and the turnover frequency of the molecular motor, the transport can be both normal ( $\alpha_{\text{eff}} = 1$ ) and anomalous ( $\alpha \leq \alpha_{\text{eff}} < 1$ ). In particular, we demonstrate in detail how highly efficient normal motor transport can emerge despite the anomalously slow passive diffusion of cargo particles, and how the active motion of the same motor in the same cell may turn anomalously slow when the parameters are changed.

*Key words:* molecular motors, anomalous Brownian motion, anomalous transport, viscoelasticity, memory effects, transport efficiency

## Introduction

Molecular transport inside biological cells comprises both passive and active processes (1). Thermal Brownian motion presents a ubiquitous mechanism especially for small particles like metal ions, aminoacids, sugar molecules, and even for larger particles like transcription factors, enzymes, RNAs, lipid granules, etc. (2). Mean squared distance covered by a particle moving randomly without any mean bias,  $\langle \mathbf{r} \rangle = 0$ , scales linearly with time,  $\langle (\delta \mathbf{r})^2 \rangle = \langle \mathbf{r}^2 \rangle - \langle \mathbf{r} \rangle^2 \propto Dt$ . If to apply a biasing external force  $\mathbf{f}_{\text{ext}}$ , the mean distance in the direction of bias scales also linearly with time,  $\langle \mathbf{r} \rangle \propto \mathbf{f}_{\text{ext}} t / \eta$ . The diffusion coefficient  $D$ , viscous friction coefficient  $\eta$ , and temperature  $T$  are related by the Einstein relation,  $D = k_B T / \eta$  ( $k_B$  is the Boltzmann constant). It manifests classical fluctuation-dissipation theorem (FDT) at local thermal equilibrium (3). The Stokes formula,  $\eta = 6\pi\zeta a$ , relates viscous friction with the medium's viscosity  $\zeta$  and radius  $a$  for spherical particles in simple fluids. The larger the particle the smaller its mobility  $\mu = 1/\eta$  and diffusion coefficient. In complex molecularly crowded polymeric fluids like cytosol this simple linear dependence on the particle's size generally breaks down and the effective friction coefficient  $\eta_{\text{eff}}$  can exponentially be enhanced in cytosol with respect to one in water by many orders of magnitude, depending on the particle size, correlation length of polymeric fluid, and other parameters (4, 5). If for a calcium ion the felt cytosol viscosity can be essentially the same as one of water, a vesicle or magnetosome with  $a > 100$  nm can feel it rather as one of glycerol (1500 $\times$  more viscous than water at room temperatures), or even honey (10000 $\times$  more viscous), as it can be guessed from recent systematic studies in (6) for a more simple system. Even for particles of a typical size of globular protein  $a \sim 2.5$  nm the enhancement factor can be as large as 750, as derived in (7) from the experimental data in (8).

Passive diffusion of submicron particles in living cells slows down tremendously, if to consider it as a normal diffusion process on macroscale, with respect to one in pure water. However, even this is not necessarily the major effect because cytosol behaves as a viscoelastic polymeric fluid displaying profound memory effects. Viscoelasticity alone can cause a subdiffusive behavior,  $\langle (\delta \mathbf{r})^2 \rangle \propto D_\alpha t^\alpha$ , with  $0 < \alpha < 1$  and subdiffusion coefficient  $D_\alpha$ , which has already been found in numerous experiments (8–25), though other subdiffusive mechanisms were also suggested to explain the experimental results (21, 23). They can also emerge in a combination with viscoelasticity, as the results in (19, 22) suggest. In particular, crowding in polymer liquids has been shown to cause namely viscoelastic subdiffusion (16, 25), which is

related to the fractional Brownian motion (26), as discussed in (27). This connection can be derived (28, 29) from a Generalized Langevin Equation, or GLE (3, 30) with a power-law decaying memory kernel and fractional Gaussian thermal noise (27, 31) as a dynamically well-founded approach with deep roots in statistical mechanics (30, 32, 33). Cytosol is a highly crowded and viscoelastic liquid, which is a common point (34, 35). This approach is used also in this work. As an example pertinent to this work, the subdiffusive motion of magnetosomes with  $a = 300$  nm and their chains (up to 8 magnetosomes in a chain) in Ref. (17) is subdiffusive with  $\alpha \approx 0.4$  in intact cytosol. It is characterized by subdiffusion coefficients as small as  $D_{0.4} \sim 10^{-16} \text{ m}^2/\text{s}^{0.4} = 100 \text{ nm}^2/\text{s}^{0.4}$ , and even smaller, depending on the number of magnetosomes in the chain. Therefore, the corresponding subdiffusional spread within one second is of the order of 10 nm only. This brings the theme of active transport by molecular motors into the focus of attention.

Without help of molecular motors such particles would be practically localized on appreciable long time scales. The motors are thus crucial for the delivery of such and similar cargos in living cells (36, 37). The theory of molecular motors viewed as Brownian stochastic engines is well developed for memoryless Markovian dynamics only, in the complete neglect of non-Markovian memory effects caused, in particular, by the viscoelasticity of cytosol. This necessitates that transport by molecular motors (38–44) in viscoelastic media should be elaborated in basic detail. We started to do this in Refs. (31, 45–49). The field of Brownian ratchets (50) is allied to molecular motors (38–42, 51), though it is dealing first and foremost with more general problems of statistical physics. Within a generalist model, one can think of the transport as one realized by the motor particle with a tightly coupled cargo making one compound particle moving in a periodic external force field provided by its interaction with microtubule (in the case of kinesins), which depends on the conformation of motor protein particle. A corresponding generalization of the standard continuous diffusion ratchet model of molecular motors towards viscoelastic subdiffusion has been put forward recently in (52). It explains a number of experimental facts, in particular, that the transport by molecular motors in viscoelastic cytosol can be both normal and anomalously slow, depending in particular on the motor operating frequency and the cargo size.

In the present work, we provide a further generalization of this recent model in (52) by considering transport of large subdiffusive cargos attached on elastic linkers to the motors. Here, the assumption of absolutely rigid linker between the motor and its cargo is relaxed. Similar models have been

considered earlier for the normal diffusion of both cargo and motor (53). The dynamics of motor is also normal in this paper, without memory effects, when it is left alone. We characterize it by a largely reduced (by a factor of 10) diffusion coefficient with respect to one expected in water. However, the coupling to subdiffusive cargo enforces the motor's subdiffusion, when it is not coupled to a microtubule. Considering experimentally relevant elastic constants of linker (18, 54) and other realistic parameters we confirm all the major features revealed in (52) in a more general setup. The anomalous transport regime becomes, however, reinforced. It emerges already for motor turnover frequencies of the order of 100 Hz for sufficiently large cargos of a typical size  $a = 300$  nm. However, even for such large cargos the transport can become normal if turnover frequency is lowered to 10 Hz. Generally, the dependence of the effective subdiffusive transport exponent on the cargo size and motor turnover frequency would make a decisive test in favor of our theory of anomalous transport mediated by molecular motors in living cells.

## Model and theory

Diffusion in such complex viscoelastic fluids as cytosol is commonly described by the Generalized Langevin Equation, or GLE (55, 56). We consider it here for overdamped dynamics, in neglect of inertial effects, written for one Cartesian coordinate  $y$  for simplicity,

$$\int_{-\infty}^t \eta_c(t-t') \dot{y}(t') dt' = f_{\text{ext}}(t) + \xi_c(t). \quad (1)$$

Here the memory kernel  $\eta_c(t)$  and the autocorrelation function of unbiased thermal colored Gaussian noise  $\xi_c(t)$  are related by the second FDT of Kubo, named also fluctuation-dissipation relation (FDR),

$$\langle \xi_c(t) \xi_c(t') \rangle = k_B T \eta_c(|t-t'|). \quad (2)$$

It reflects the energy balance at thermal equilibrium between the energy pumped by thermal noise and energy dissipated due to friction. Such a stochastic description is not only consistent with the laws of equilibrium statistical physics and thermodynamics, but it also allows to treat strongly out-of-equilibrium transport, driven e.g. by a non-thermal fluctuating force  $f_{\text{ext}}(t)$ . GLE 1 serves as a basis in passive microrheology (11, 55, 56), at thermal equilibrium, to derive the complex shear modulus of the medium in the frequency domain,  $G^*(\omega) \propto i\omega \int_0^\infty \exp(-i\omega t) \eta(t) dt$ , from the particle

trajectories. The complex shear modulus is commonly used to characterize viscoelastic materials (57). In particular, a frequently observed power law scaling  $G^*(\omega) \propto (i\omega)^\alpha$  with  $0 < \alpha < 1$  corresponds to subdiffusion,  $\langle(\delta x)^2\rangle \propto D_\alpha t^\alpha$ , with fractional diffusion coefficient  $D_\alpha$  and power law scaling of memory decay,  $\eta(t) \propto \eta_\alpha/t^\alpha$ , where  $\eta_\alpha$  is fractional friction coefficient obeying fractional Einstein relation  $D_\alpha = k_B T/\eta_\alpha$  (31). In macroscopic theory of viscoelasticity, similar memory kernels were introduced long ago by A. Gemant (58) as a generalization of the simplest Maxwell model with exponentially decaying memory (59). In practice, such a power law scaling extends mostly over several time and frequency decades. High-frequency (short-memory) cutoff reflects molecular nature of the condensed medium. A low-frequency, or long-memory cutoff guarantees that the macroscopic friction coefficient  $\eta_{\text{eff}} = \int_0^\infty \eta(t)dt$  is finite, which reflects finite viscosity of any fluid on macroscale (27, 31). Intermediate power law scaling gives rise to subdiffusion on a transient time scale (up to several minutes, depending on the particle's size), and this can establish subdiffusion as a primary passive transport mechanism for submicron particles on the mesoscale of biological cells interior.

The mathematical model of a strictly algebraically decaying memory kernel corresponds to the fractional Gaussian noise (fGn) model of thermal noise. fGn presents a time-derivative of the fractional Brownian motion (fBm) (26). Both can be characterized by the Hurst exponent  $H' = 1 - \alpha/2$ . Such a noise is persistent for  $1/2 < H' < 1$ , with positive correlations. It corresponds to the sub-Ohmic model of thermal baths consisting of harmonic oscillators (60). The corresponding GLE can be derived from a purely dynamic hyper-dimensional Hamiltonian model assuming merely initial canonical distribution of thermal bath oscillators at a given temperature, like in a typical molecular dynamics setup (30, 60). It has thus the firm statistic-mechanical foundation. The solution of GLE 1 is then also fBm, but anti-persistent and subdiffusive, with the Hurst exponent  $H = \alpha/2$ . This transformation occurs due to the friction with algebraically decaying memory (29). Important, this is namely the memory friction which is at the heart of the very phenomenon of viscoelasticity. Experimental values of  $\alpha$  can be very different, in the range of  $\alpha = 0.2 \div 1$  (23). For example, for the intact cytoskeleton in Ref. (17),  $\alpha = 0.4$ . About the same value can be derived from the experimental data in Ref. (18), namely from the power spectrum  $S(\omega)$  of the transversal position fluctuations of the melanosome particles (size  $a = 250$  nm) elastically attached to the motor proteins walking along microtubule. For sufficiently large frequencies (exceeding inverse relaxation time scale in parabolic potential well),  $S(\omega) \propto 1/\omega^b$ , with  $b = 1 + \alpha$  and

experiment yields  $b = 1.41 \pm 0.02$ . We accept  $\alpha = 0.4$  as an experimentally relevant numerical value in this work.

### Earlier modeling

The simplest idea to model the influence of molecular motors on the cargo dynamics within the GLE approach is to approximate their collective influence by a time-dependent random force  $f_{\text{ext}}(t)$ , which itself exhibits a long range memory and is power law correlated,  $\langle f_{\text{ext}}(t')f_{\text{ext}}(t) \rangle \propto 1/|t - t'|^\gamma$ , with  $0 < \gamma < 1$ . This can lead to superdiffusion (61),  $\langle (\delta y)^2 \rangle \propto t^\beta$ , with  $\beta = 2\alpha - \gamma > 1$  (28, 61), for  $\alpha > 0.5$ . Notice, however, that  $\beta$  can take the maximal value of  $2\alpha$ , for  $\gamma \rightarrow 0$ , within this model. This corresponds to a strict  $1/f$  noise driving force  $f_{\text{ext}}(t)$  generated by motors with almost non-decaying correlations. The origin of this limit can easily be understood, if to consider the transport by a time-alternating force  $\pm f_0$  in the opposite directions. Then,  $\langle \delta y(t) \rangle \propto \pm f_0 t^\alpha$ , for a force realization, and after averaging over the driving force fluctuations  $\langle \langle \delta y(t) \rangle^2 \rangle_{f_0} \propto t^{2\alpha}$ . Any decaying correlations of the alternating driving force make the effective diffusion exponent smaller than  $\beta_{\text{max}} = 2\alpha$ . Clearly, within such a description superdiffusion caused by the activity of molecular motors could only be possible for  $\alpha > 0.5$ , at odds with experimental results showing  $\beta \sim 1.2 \div 1.4$  for  $\alpha = 0.4$  (17). Such a model is therefore too simple. It cannot explain some important experimental findings consistently, providing but a useful first insight.

### Our model

We consider thus a further generalization, where the cargo is elastically coupled to the motor with coordinate  $x$  (one-dimensional model), and  $f_{\text{ext}} = k_L(x - y)$ , with spring constant  $k_L$ . The motor undergoes diffusion, generally characterized by a memory friction  $\eta(t)$ , on microtubule in a binding potential  $U(x, \zeta(t))$  reflecting spatial period  $L$  of microtubule. The potential depends on the dynamical motor conformation  $\zeta(t)$ , the motor's internal degree of freedom. Our model reads,

$$\int_{-\infty}^t \eta_c(t - t') \dot{y}(t') dt' = -k_L(y - x) + \xi_c(t), \quad (3)$$

$$\int_{-\infty}^t \eta(t - t') \dot{x}(t') dt' = k_L(y - x) - \frac{\partial}{\partial x} U(x, \zeta(t)) - f_0 + \xi(t), \quad (4)$$

where the memory kernels and the autocorrelation functions of unbiased thermal colored Gaussian noises are related by FDRs 2, and  $\langle \xi(t)\xi(t') \rangle = k_B T \eta(|t-t'|)$ ;  $\xi_c(t)$ , and  $\xi(t)$  are not correlated.  $f_0$  in 4 is a constant loading external force which can oppose the fluctuation-induced transport and stop it. We assume further that dynamical conformation  $\zeta(t)$  can take two values  $\zeta_1$  and  $\zeta_2$ . The binding potential is periodic,  $U(x+L, \zeta_{1,2}) = U(x, \zeta_{1,2})$ , but spatially asymmetric, see in Fig. 1, lower inset. Spatial periodicity guarantees that transport is absent in the absence of conformational fluctuations induced by ATP binding to molecular motor and its hydrolysis. It is forbidden by the symmetry of thermal detailed balance, at thermal equilibrium, in the absence of an energy source. We assume that two consequent conformational switches make one cycle, and  $U(x+L/2, \zeta_1) = U(x, \zeta_2)$ . Switching between two conformations is considered as symmetric two-state Markovian process with the equal transition rates  $2\nu_{\text{turn}}$ .

To be more specific, one considers piecewise linear sawtooth potential (piecewise constant potential force) with amplitude  $U_0$  and period  $L$ . The minimum divides the period in the ratio  $p : 1$ , and we take a particular value  $p = 3$ . This asymmetry defines the natural direction of transport towards positive  $x$ . The maximally possible loading, or stalling force for this potential at zero temperature is easy to deduce:  $f_0^{\text{stop}}(T = 0) = (p + 1)U_0/(pL)$ . In units of room  $k_B T_r = 4.1 \cdot 10^{-21} \text{ J} = 4.1 \text{ pN} \cdot \text{ nm}$ ,  $L = 8 \text{ nm}$ , and  $f_0^{\text{stop}}(T = 0) \approx 0.6833 U_0/(k_B T_r) \text{ pN}$  for  $p = 3$ . For  $T = T_r$  it will be essentially lower, see below. We choose  $U = 20 k_B T_r$  in our simulations. This corresponds to  $f_0^{\text{stop}}(T = 0) = 13.67 \text{ pN}$ , about twice the maximal loading force of kinesin II at physiological temperatures.

In this work, we neglect the memory effects for the motor particle,  $\eta(t) = 2\eta_m \delta(t)$ , with Stokes friction  $\eta_m = 6\pi a_m \zeta_w$ , where  $a_m$  is the effective radius of motor molecule and  $\zeta_w = 1 \text{ mPa} \cdot \text{ s}$ . We take  $a_m = 100 \text{ nm}$ , about 10 times larger than a linear geometrical size of kinesin in order to account for the enhanced effective viscosity felt by the motor in cytosol with respect to its water constituent. A characteristic time scale  $\tau_m = L^2 \eta_m / U_0^*$  has been used for scaling time in numerical simulations, with  $U_0^* = 10 k_B T_r$ . For the stated parameters,  $\tau_m \approx 2.93 \mu\text{s}$ . Distance is scaled in units of  $L$ , and elastic coupling constants in units of  $U_0^*/L^2 \approx 0.64 \text{ pN/nm}$ . Next, we single out purely viscous component in the memory kernel  $\eta_c(t) = 2\eta_c \delta(t) + \eta_{\text{mem}}(t)$ , where  $\eta_{\text{mem}}(t) = \eta_\alpha / (\Gamma(1 - \alpha)t^\alpha)$ .

If the cargo is uncoupled from the motor ( $k_L \rightarrow 0$ ), its diffusional behavior is described by (49)

$$\langle \delta y^2(t) \rangle = 2D_c t E_{1-\alpha, 2} \left( -(t/\tau_{\text{in}})^{1-\alpha} \right), \quad (5)$$

where  $E_{a,b}(z) = \sum_{n=0}^{\infty} z^n / \Gamma(an + b)$  is generalized Mittag-Leffler function,  $D_c = k_B T / \eta_c$  is normal diffusion coefficient, and  $\tau_{\text{in}} = (\eta_c / \eta_\alpha)^{1/(1-\alpha)}$  is a time constant separating initially normal diffusion,  $\langle \delta y^2(t) \rangle \approx 2D_c t$  at  $t \ll \tau_{\text{in}}$ , and subdiffusion,  $\langle \delta y^2(t) \rangle \approx 2D_\alpha t^\alpha / \Gamma(1 + \alpha)$  for  $t \gg \tau_{\text{in}}$ . Furthermore, in accordance with the methodology in (27, 31) we approximate the memory kernel by a sum of exponentials

$$\eta_{\text{mem}}(t) \approx \eta_{\text{mem}}(t, \nu_0, b, N) = \sum_{i=1}^N k_i \exp(-\nu_i t), \quad (6)$$

obeying a fractal scaling,  $\nu_i = \nu_0 / b^{i-1}$ ,  $k_i \propto \nu_i^\alpha$ . This form ensures a power law scaling,  $\eta_{\text{mem}}(ht, \nu_0, b, N) = h^{-\alpha} \eta_{\text{mem}}(t, h\nu_0, b, N)$ , for  $t$  being well within the time-interval between two cutoffs,  $\tau_{\text{min}} = \nu_0^{-1}$  and  $\tau_{\text{max}} = \tau_{\text{min}} b^{N-1}$ . The dilation parameter  $b > 1$  controls the accuracy of approximation, which exhibits small logarithmic oscillations with respect to the exact power law, and  $\nu_0$  corresponds to a high-frequency cutoff reflecting atomic/molecular nature of any physical condensed environment. In this respect, any physical fractal, either spatial or in time, has minimal and maximal ranges, defined in our case by the ratio  $\tau_{\text{max}} / \tau_{\text{min}} = b^{N-1}$ , and even a rough decade scaling with  $b = 10$  allows to approximate the power law with accuracy of several percents for  $\alpha = 0.4$  (further increased to a one hundredth of percent for  $b = 2$  (48)). Similar expansions are well known in the theory of anomalous relaxation (62). This provides a foundation for excellent numerical method to integrate fractional GLE dynamics. Alternatively, this methodology can be considered as an independent approach to model anomalous diffusion and transport on physically relevant spatial and time scales, not caring much about its relation to fractional GLE. Then, a convenient parameterization is

$$k_i = \nu_0 \eta_{\text{eff}} \frac{b^{1-\alpha} - 1}{b^{(i-1)\alpha} [b^{N(1-\alpha)} - 1]}, \quad (7)$$

where  $\int_0^\infty \eta_{\text{mem}}(t) dt = \eta_{\text{eff}}$  characterizes largely enhanced macroscopic friction coefficient in a long-time limit,  $t \gg \tau_{\text{max}}$ . The number  $N$  of auxiliary quasi-particles controls the maximal range of subdiffusive dynamics, which becomes again normal,  $\langle \delta y^2(t) \rangle \sim 2D_{\text{eff}} t$ , for  $t \gg \tau_{\text{max}}$  with  $D_{\text{eff}} = k_B T / (\eta_{\text{eff}} + \eta_c)$ . Notice that the fractional friction coefficient is related to the effective friction as  $\eta_\alpha = \eta_{\text{eff}} \tau_{\text{max}}^{\alpha-1} / r$ . Here,  $r = \frac{C_\alpha(b)}{\Gamma(1-\alpha)} \frac{b^{1-\alpha}}{b^{1-\alpha}-1} [1 - b^{-N(1-\alpha)}]$  is a numerical coefficient of the order of unity,  $r \approx 0.93$  for  $N \geq 5$ , at  $\alpha = 0.4$ , and  $b = 10$ , with  $C_{0.4}(b) \approx 1.04$ . The effective relative friction coefficient

$\tilde{\eta}_{\text{eff}} = \eta_{\text{eff}}/\eta_c$  is used as an important parameter in our simulations. It defines the time range of subdiffusion, from  $\tau_{\text{in}} = \tau_{\text{max}}/\tilde{\eta}_{\text{eff}}^{1/(1-\alpha)}$  to  $\tau_{\text{max}}$ . For example, for  $\tilde{\eta}_{\text{eff}} = 10^3$  and  $\alpha = 0.4$  one expects that subdiffusion will extend over 5 time decades. According to this important, nontrivial but simple relation, the relative increase of effective friction controls the relative time range of subdiffusion  $\tilde{\eta}_{\text{eff}}^{1/(1-\alpha)}$ , independently of  $b$ , and  $N$ !

The discussed approximation allows to replace the non-Markovian GLE dynamics with a higher dimensional Markovian dynamics upon introduction of the  $N$  auxiliary Brownian quasi-particles with coordinates  $y_i$  accounting for viscoelastic degrees of freedom, see in (31) for details. In the present case,

$$\begin{aligned} \eta_m \dot{x} &= f(x, \zeta(t)) - k_L(x - y) + \sqrt{2\eta_m k_B T} \xi_m(t), \\ \eta_c \dot{y} &= k_L(x - y) - \sum_{i=1}^N k_i(y - y_i) + \sqrt{2\eta_c k_B T} \xi_0(t), \\ \eta_i \dot{y}_i &= k_i(y - y_i) + \sqrt{2\eta_i k_B T} \xi_i(t), \end{aligned} \quad (8)$$

where  $f(x, \zeta(t)) = -\partial U(x, \zeta(t))/\partial x - f_0$ , and  $\eta_i = k_i/\nu_i$ . Furthermore,  $\xi_i(t)$  are uncorrelated white Gaussian noises of unit intensity,  $\langle \xi_i(t') \xi_j(t) \rangle = \delta_{ij} \delta(t - t')$ , which are also uncorrelated with white Gaussian noises  $\xi_0(t)$  and  $\xi_m(t)$ . To have a complete equivalence with the stated GLE model in Eqs. 3-6, the initial positions  $y_i(0)$  are sampled from a Gaussian distribution centered around  $y(0)$ ,  $\langle y_i(0) \rangle = y(0)$  with variances  $\langle [y_i(0) - y(0)]^2 \rangle = k_B T/k_i$ . The stochastic variable  $\zeta(t)$  is described by a symmetric two-state Markovian process with the identical transition rates  $\nu = 2\nu_{\text{turn}}$ . This corresponds to the simplest model of molecular motors considered as flashing ratchets (1, 38, 42). By doing numerical solutions of the set 8 with a time step  $\delta t \ll \nu^{-1}$ , the variable  $\zeta(t)$  alternates its state with the probability  $\nu \delta t$  at each integration time step, or continues to stay in the same state with probability  $1 - \nu \delta t$ . This is decided upon comparison of a (pseudo)-random number uniformly distributed between zero and one with  $\nu \delta t$ .

## Thermodynamic efficiency and energetic efficiency of the cargo delivery

Thermodynamic efficiency of anomalous Brownian motors has been addressed quite recently (48, 49). It turns out that the general approach developed earlier for normal motors (39, 63) can be almost straightforwardly applied. It yields, however, several important new results in the anomalous

transport regime. Generically, the work done by the potential fluctuations induced by the enzyme turnovers, or the input energy pumped into directed motion is  $E_{\text{in}}(t) = \int_0^t \frac{\partial}{\partial t} U(x, t) dt$  (63). It can be further calculated, within the considered model, as a sum of potential energy jumps  $\Delta U(x(t_i))$  occurring at random instants of time  $t_i$  marking cyclic conformational transitions  $1 \rightarrow 2 \rightarrow 1 \rightarrow \dots$ . This input energy is spent on doing work against external loading force  $f_0$ . The corresponding useful work is  $W_{\text{use}}(t) = f_0 \delta x(t)$ . The rest is used to overcome the dissipative influence of environment. It is dissipated as heat. The thermodynamic efficiency of isothermal motors is thus just  $R_{\text{th}}(t) = \langle W_{\text{use}}(t) \rangle / \langle E_{\text{in}}(t) \rangle$ , upon averaging over many ensemble realizations. Clearly,  $R_{\text{th}} = 0$  for  $f_0 = 0$ . This is also very clear from an energetic point of view as by relocation from one place to another neither potential energy of cargo, nor that of motor has been changed. This is a normal *modus operandi* of such motors as kinesin which is very different from other molecular machines such as ion pumps which are primarily transferring ions against an electrochemical potential gradient, i.e. increase electrochemical potential of ions. Anomalously slow transport introduces principally new features for  $f_0 > 0$ . Namely, for anomalous transport the useful work done against  $f_0$  scales sublinearly with time,  $\langle W_{\text{use}}(t) \rangle \propto f_0 t^{\alpha_{\text{eff}}}$ , while the input energy scales linearly,  $\langle E_{\text{in}}(t) \rangle \propto t$ . It is proportional to the mean number of potential fluctuations. By the some token as fractional transport cannot be characterized by a constant mean velocity, it cannot be also characterized by mean power of useful work in a stationary regime. However, one can define fractional power and fractional efficiency (48, 49). Thermodynamic efficiency simply does not present a completely adequate measure in such a situation. Nevertheless, it decays algebraically slow in time,  $R_{\text{th}}(t) \propto 1/t^{1-\alpha_{\text{eff}}}$  and can be still rather high even for large times, see below. Moreover, the dependence of  $R_{\text{th}}(t, f_0)$  on load  $f_0$  is also very illustrative,  $R_{\text{th}}(t, f_0)$  vanishes not only at  $f_0 = 0$ , but also at some  $f_0^{\text{stop}}(T, U_0, \nu_{\text{turn}})$ . It defines the stalling force, which is time-independent, but strongly depends on the potential amplitude, temperature, and driving frequency, as will be shown also below. Thermodynamic efficiency has thus a maximum at some optimal loading force  $f_0^{\text{opt}}(t)$ , and  $R_{\text{th}}(t, f_0^{\text{opt}})$  can be in anomalous transport regime still very high, for a sufficiently high  $U_0$ , comparable with the maximal thermodynamic efficiency of kinesins in normal regime of about 50%. The dependence of  $R_{\text{th}}(t, f_0)$  on  $f_0$  is strongly asymmetric in a thermodynamically highly efficient regime. However, it becomes more symmetric in a low efficient anomalous regime, where it is described approximately by a parabolic dependence,  $R_{\text{th}} \propto f_0(1 - f_0/f_0^{\text{stop}})/f_0^{\text{stop}}$  with  $f_0^{\text{opt}} = f_0^{\text{stop}}/2$ , and a proportionality coefficient which slowly drops in time.

This phenomenon of a time-dependence of  $R_{\text{th}}(t)$  can be verbalized as fatigue of molecular motors caused by viscoelasticity of cytosol. It can be considered as one of indications in the favor of our theory if revealed experimentally. In the anomalous transport regime asymptotically  $R_{\text{th}}(t) \rightarrow 0$  independently of  $f_0$ . Even though the useful work done against  $f_0$  is always finite, which is a benchmark of any genuine Brownian motor, it becomes a negligible portion of input energy in the course of time. The input energy is spent mostly to overcome the dissipative influence of the environment with hugely enhanced effective viscosity, which is quite natural. It is dissipated as heat,  $Q(t) = \langle E_{\text{in}}(t) \rangle - \langle W_{\text{use}}(t) \rangle$ .

However, the primary utility of such motors as kinesin consists in delivery various cargos to certain destinations and not in increasing their potential energy. For this reason, numerous Stokes efficiencies have been defined in addition to  $R_{\text{th}}$  (64–66). Which of them is most appropriate remains dim, especially for anomalous transport (49). We proposed a different measure to quantify the motor performance at  $R_{\text{th}} = 0$  named energetic delivery performance (52). It reflects optimization of the mean delivery velocity per energy spent. If to quantify the net input energy in the number of enzyme turnovers (number of ATP molecules consumed as fuel), a natural definition is  $D = d/(t\langle N_{\text{turn}} \rangle)$ , where  $d$  is the delivery distance in time  $t$ , after  $\langle N_{\text{turn}} \rangle$  cyclic turnovers on average. Clearly,  $\langle N_{\text{turn}} \rangle = \nu_{\text{turn}}t$ , and for an ideal motor in the tight coupling power stroke regime, whose processive motion is perfectly synchronized with the turnovers of “catalytic wheel” (67),  $d = L\nu_{\text{turn}}t$ , and therefore  $D_{\text{ideal}} = L^2\nu_{\text{turn}}/d$ , i.e. for any given  $d$ , the increase of  $\nu_{\text{turn}}$  leads to a linearly increased delivery performance. Clearly, in reality there will be always deviations from this idealization. With increasing turnover frequency, or upon increasing load even normally operating motors have not enough time to relax down potential minimum after each potential jump, or escape events become important. This results in backsteps, and after reaching a maximum versus  $\nu_{\text{turn}}$  the delivery efficiency will necessarily drop. In the anomalous transport regime, the larger the delivery distance  $d$  the smaller the corresponding optimal  $\nu_{\text{turn}}^{\text{opt}}(d)$ . Energetically, it makes less sense to hydrolyze more ATP molecules for the efficient cargos delivery. A corresponding optimization can be important in the cell economy.

## Results

We use in our simulations  $N = 10$ ,  $b = 10$ , and  $\nu_0 = 100$  yielding  $\tau_{\text{max}} \approx 29.4$  s for  $\tau_m = 2.94 \mu\text{s}$ . Numerical solution of stochastic differential equations 8

was done implementing stochastic Heun method (68) in CUDA on NVIDIA Kepler graphical processor units. Time-step of integration was  $\delta t = 5 \cdot 10^{-3}$  in the scaled units and the terminal time was  $10^6$  (2.94 s) in most simulations. We considered a cargo with  $a = 300$  nm ( $\eta_c/\eta_m = 3$ ) and two different values of  $\tilde{\eta}_{eff} = 3 \cdot 10^4$  (which we shall name “larger”) and  $\tilde{\eta}_{eff} = 3 \cdot 10^3$  (“smaller”). This corresponds to two different values of subdiffusion coefficient  $D_\alpha^{(1)} \approx 171$  nm<sup>2</sup>/s<sup>0.4</sup>, in accordance with typical values measured for magnetosomes in (17) and ten times larger  $D_\alpha^{(2)} \approx 1710$  nm<sup>2</sup>/s<sup>0.4</sup> which can be attributed to a smaller particle. Furthermore, two different values of elastic spring constant were used  $k_L^{(1)} = 0.32$  pN/nm (“strong”), which corresponds to measurements in vitro (54), and a ten times softer  $k_L^{(2)} = 0.032$  pN/nm (“weak”) in accordance with the recent results in (18), in living cells. Furthermore,  $\nu_{\text{turn}}^{(1)} = 85$  Hz and  $\nu_{\text{turn}}^{(2)} = 17$  Hz denote two turnover frequencies (“fast” and “slow”). Five different sets of parameters, labeled as  $S_1, S_2, S_3, S_4, S_5$  correspond to “larger cargo, stronger linker, fast”, “smaller cargo, stronger linker, fast”, “smaller cargo, weaker linker, fast”, “larger cargo, weaker linker, fast”, and “larger cargo, stronger linker, slow”, respectively.

First, we illustrate a single trajectory realization of anomalous transport for the set  $S_1$  in Fig. 1, a. The upper inset in this figure shows the coupled diffusion of the cargo and the motor off the microtubule track. Without any coupling, the motor particle diffuses normally on any time scale within the considered model, and the cargo initially diffuses normally as well, but then it subdiffuses until the time scale  $\tau_{\text{max}}$  is reached. Here, a time-averaging of the particle position variances  $\delta x^2(t|t') = [x(t+t') - x(t')]^2$  over the corresponding single trajectories (time-averaging over sliding  $t'$  within a time window  $\mathcal{T}$ ) is done,  $\overline{\delta x^2(t)} = \frac{1}{\mathcal{T}-t} \int_0^{\mathcal{T}-t} \delta x^2(t|t') dt'$  ( $t \ll \mathcal{T}$ ). It coincides with the ensemble-average  $\langle \delta x^2(t) \rangle$  since the considered viscoelastic diffusion is ergodic (27). As it is clearly seen from Fig. 1, a, the coupled motor and cargo subdiffuse together  $\langle \delta x^2(t) \rangle \propto t^\alpha$  after some transient time. In other words, subdiffusing particle enslaves the normally diffusing one, when the last one is passive and not empowered by trapping and pulsing potential. There is no mean displacement of this complex on average. However, when the motor is attached to the track, it processively steps in the direction defined by the potential asymmetry, and the (freely) subdiffusing cargo cannot withstand. It follows to the winning motor. Initially, the motor steps are perfectly tight to the potential fluctuations (notice that a particular realization of the counting process in units of  $L/2$  in this figure is faster than the

average value corresponding to the optimal transport distance  $d = L\nu_{\text{turn}}^{(1)} t$ , cf. the broken line). After some initial time one can clearly see backsteps of the motor and cargo is always fluctuating around the motor position. However, it lags somewhat behind the motor on average. It is not obvious from this figure that the transport is anomalously slow and not just corresponds to some suboptimal mean motor velocity  $v < v_{\text{opt}} = L\nu_{\text{turn}}$ . However, the transport is anomalous indeed,  $\langle \delta x(t) \rangle \propto t^{\alpha_{\text{eff}}}$ , as it can be deduced after averaging over 1000 different trajectory realizations. This allows to deduce the anomalous transport exponent  $\alpha_{\text{eff}}$ . As already verified in our previous studies of viscoelastic subdiffusive dynamics in periodic non-linear potentials, such  $\alpha_{\text{eff}}$  is generally time-dependent. However, it relaxes to a long-time limiting value in the course of time, which is displayed in Fig. 2 as function of load  $f_0$  for different sets of parameters. For  $S_1$  and  $f_0 = 0$  in Fig. 1, a,  $\alpha_{\text{eff}} \approx 0.7$ . This explains the origin of superdiffusive exponent  $\beta = 1.4$ , in spite of the low value of free subdiffusion exponent  $\alpha = 0.4$  in (17). However, for a smaller particle (or rather for a smaller  $\eta_\alpha$  in our model), the case  $S_2$ , the transport becomes normal at the same flashing frequency and without biasing back load,  $f_0 = 0$ , see in Fig. 1, b. Interestingly, the corresponding single trajectory realization in Fig. 1, b does not correspond to a larger transport distance at  $t = 1$  s, maximal in this figure, as compare with anomalous transport in Fig. 1, a. This is simply because the number of turnovers done until this time is larger in Fig. 1, a than in Fig. 1, b, for the particular realizations presented. This reflects statistical variation of the corresponding counting process, or, in physical terms, stochastic nature of single motor proteins. A perfect synchronization between the potential switches and the motor steps makes the orange line corresponding to the potential switches barely visible in Fig. 1, b. One can see also in the upper inset that cargo fluctuates around the motor symmetrically. It does not lag behind the motor on average, like in Fig. 1, a. Furthermore, a much softer linker does not change qualitatively the results, as Fig. 2 demonstrates, though anomalous transport is stronger affected. Unexpectedly,  $\alpha_{\text{eff}}$  is slightly larger for a softer linker at  $f_0 = 0$  in the anomalous regime. This is because we derived  $\alpha_{\text{eff}}$  from the position of the motor, rather than cargo and the enlarged mean distance between the motors and their cargos was still not completely relaxed to a stationary value for  $S_4$  in Fig. 2. Moreover, the anomalous transport can become normal if the turnover frequency is reduced, see the results for  $S_5$  in Fig. 2. These results show that motors can realize both normal and anomalous transport in viscoelastic cytosol of living cells, where the large particles sub-

diffuse on the time scale from milliseconds to seconds. Which regime will be realized depends in particular on the particle size (or fractional friction coefficient  $\eta_\alpha$ ) and the enzyme turnover frequency  $\nu_{\text{turn}}$ , but only weakly depends on the linker rigidity. This presents one of the important results of our work. Furthermore, if to apply a counter-force  $f_0 > 0$ , the anomalous transport regime becomes promoted, cf. in Fig. 2. This effect is primarily due to reduction of the binding potential amplitude  $U_0$ . Anomalous transport will also emerge immediately for the studied parameters if to decrease  $U_0$  essentially, e.g. to  $10 k_B T_r$ .

The transport efficiency of molecular motors in viscoelastic cytosol can be almost perfect, despite subdiffusion, as Fig. 3 demonstrates for  $S_2$  and realistic turnover frequencies (lower than 200 Hz) even for large distances like  $8 \mu m$ . The discussed power stroke mechanism can perfectly overcome subdiffusive resistance of medium, if the cargo size is not too large. In anomalous transport regime with strongly decreased transport efficiency there exists but an optimal turnover frequency, which depends on the delivery distance. Interestingly, this optimization does not depend manifestly on the rigidity of linker, see in Fig. 3. However, anomalous transport on a stronger linker is yet more efficient for realistic turnover frequencies. And this agrees with our intuition.

Thermodynamic efficiency becomes strongly affected by the fact that an increase of  $f_0$  promotes anomalous transport regime, see in Fig. 2. Even if the transport was normal at  $f_0$ , it becomes anomalous under sufficiently strong external load  $f_0$ . Hence thermodynamic efficiency starts to depend on time and it vanishes asymptotically, whenever the transport is anomalous. However, it can be substantially large even at large times such as  $t_{\text{max}} \sim 3$  s in Fig. 4, where it is still about 23% at maximum, see results for  $S_2, S_3$ , where thermodynamic efficiency practically does not depend on the linker rigidity. For low efficient anomalous transport, the dependence of  $R_{\text{th}}$  on load is approximately parabolic with maximum at  $f_0^{\text{opt}} = f_0^{\text{stop}}/2$ . Counterintuitively, it is slightly larger for softer linker in Fig. 4. This is because the useful work has been defined as one done by motors against  $f_0$ , and not by cargos, and the motors step ahead their cargos on slightly larger distances for a softer linker. The maximal loading, or stalling force  $f_0^{\text{stop}}$  is time-independent. It also does not depend on the cargo size. However, it strongly depends on the flashing frequency (see in Fig. 4), and also on the potential amplitude and temperature, see in Fig. 5 for a fixed  $\nu_{\text{turn}} = 85$

Hz. Numerical results shows that for  $U_0 > U_m(\nu_{\text{turn}})T/T_r$ ,

$$f_0^{\text{stop}}(T, U_0, \nu_{\text{turn}}) \approx \frac{4}{3L} \left( U_0 - U_m(\nu_{\text{turn}}) \frac{T}{T_r} \right), \quad (9)$$

where fit to numerical data yields  $U_m \approx 11.2 k_B T_r$  at  $\nu_{\text{turn}} = 85$  Hz. The corresponding stalling force  $f_0^{\text{stop}} \approx 6$  pN for  $U_0 = 20 k_B T_r$ , but it is smaller for  $\nu_{\text{turn}} = 17$  Hz, see in Fig. 4. From this one can conclude that a reasonably strong motor requires binding potential amplitudes larger than ten  $k_B T$ . The result in Eq. 9 allows for a physical interpretation upon introduction of an effective free energy barrier  $F_0(T) = U_0 - TS_0$  with an effective ‘‘entropy’’  $S = U_m(\nu_{\text{turn}})/T_r$ . Then,  $f_0^{\text{stop}}(T, U_0, \nu_{\text{turn}}) \approx 4F_0(T)/3L$ , for positive  $F_0$ .

## Discussion and Conclusions

In this work, we elaborated on a model of active molecular transport realized by molecular motors in the case when their cargos are subdiffusing when left alone. Subdiffusion is described by a Generalized Langevin Equation with a memory kernel which scales in accordance with a power law between two memory cutoffs. Subdiffusion is realized until the long-time memory cutoff  $\tau_{\text{max}}$  is reached, and the time range of subdiffusion is determined by this time and an effectively enhanced relative (with respect to water) cytosol viscosity  $\zeta_{\text{rel}}$ , which depends on the particle size. The effective viscosity defines asymptotically normal diffusion regime, and initially diffusion is also normal. Subdiffusion occurs on the time scale between  $\tau_{\text{in}} = \tau_{\text{max}}/\zeta_{\text{rel}}^{1/(1-\alpha)}$  and  $\tau_{\text{max}}$ , and it can occur over about 6 to 7 time decades for  $\zeta_{\text{rel}} \sim 10^4$ , or about 5 time decades for  $\zeta_{\text{rel}} \sim 10^3$ , and  $\alpha = 0.4$ . Such transient subdiffusion allows for a nice multidimensional Markovian embedding with a well-controlled accuracy of approximation by using a set of overdamped Brownian quasi-particles elastically attached to cargo on harmonic springs, with spring constants and frictional coefficients obeying a fractal scaling. The molecular motor is described by a variant of standard model of flashing Brownian motors with a periodic saw-teeth potential randomly fluctuating between two realizations differing by phase, so that two potential fluctuations corresponding to one completed enzyme cycle can promote the motor by one spatial period. This model describes, in particular, a perfect power stroke ratchet transport in the case of highly processive molecular motors with binding potential amplitude exceeding a minimal height of the order of  $10 k_B T_r$ , see in Fig. 5, with  $U_0 = 20 k_B T_r$  in this work. A perfect transport regime with maximal transport efficiency emerges when the motion of motor

is locked to the potential fluctuations caused by the change of the internal motor state. The cargo is coupled elastically to the motor. This model differs profoundly from two previous modeling routes to describe active anomalous transport and diffusion in living cells. In a simplest model, the influence of motors is modeled by random force exhibiting weakly decaying correlations. It cannot, however, explain the origin of the observed superdiffusion in the cells with the passive subdiffusion exponent less or equal  $\alpha = 0.5$ , like  $\alpha = 0.4$  detected in Refs. (17, 18) and used also in this work. A better model has been introduced recently in (52). It assumes, however, a perfectly rigid linker between the motor and the cargo, like most models of molecular motors do, so that the cargo and the motor make one effectively subdiffusing (when it is left alone) Brownian particle moving in a flashing potential. That one is a model of anomalous Brownian motors. The crucial point which it explains is how one and the same motor, in the same cell can realize both normal and anomalous transport. The occurrence of particular transport regime depends on the binding potential amplitude, fractional frictional strength  $\eta_\alpha$  (depending on the cargo size), loading external force  $f_0$ , and enzyme turnover frequency. The effective transport exponent  $\alpha_{\text{eff}}$  can vary from  $\alpha$  to one, and this can easily explain the emergence of anomalously fast diffusion with  $\beta = 2\alpha_{\text{eff}}$  mediated by motors in the cells with  $\alpha \leq 0.5$ . Strikingly enough, the transport can be not only normal (in agreement with most experiments), but also reflect an almost perfect synchronization between the enzymatic turnovers and the motor's stepping along microtubule. This can be rationalized within a power-stroke mechanism and explains how a power-stroke like operation can beat subdiffusion.

The major advance of this work is the clarification of how this picture is modified upon considering realistically soft linkers between the motor (operating normally in the absence of cargo, in neglect of viscoelastic memory effects) and the subdiffusing cargo. It turns out that all the major features revealed in (52) survive, qualitatively all the results look similar. However, anomalous transport regime can emerge already for turnover frequencies less than 100 Hz (about maximal frequency for kinesin motors) and the cargo sizes about  $a = 300$  nm. We believe that these new results will inspire an experimental verification, because they should survive also in more complicated models of molecular motors operating in viscoelastic cytosol. We hope that this can be done in a nearest future.

## Figure Legends

### Figure 1.

Positions of motor (black line) and cargo (blue line) versus time for a single trajectory realization in the case of anomalous transport (part a, set  $S_1$ ,  $\tilde{\eta}_{\text{eff}} = 3 \cdot 10^4$ , see text for the parameters corresponding to various sets  $S_i$ ) and normal transport (part b, set  $S_2$ ,  $\tilde{\eta}_{\text{eff}} = 3 \cdot 10^3$ ). Turnover frequency  $\nu_{\text{turn}} = 85$  Hz. The realizations of counting process (number of potential switches multiplied with potential half-period  $L/2$ ) are depicted by orange lines (difficult to detect in part **b** because of a perfect synchronization). The broken black lines depict the dependence of the averaged (over many trajectory realizations) position of motor on time in the case of a perfect synchronization (ideal power stroke like mechanism). Upper inset in the part **a**, shows diffusion of coupled motor and cargo in the absence of binding potential. The position variances have been obtained using a corresponding single-trajectory time averaging, as described in the text. The upper inset in the part **b** magnifies a part of motor and cargo trajectories making the step-wise motion of motor obvious. It is perfectly synchronized with the potential switches. Cargo randomly fluctuates around the motor position. The lower insets show two conformations of binding potential.

### Figure 2.

Effective transport exponent  $\alpha_{\text{eff}}$  as function of loading force  $f_0$  for various sets of parameters.

### Figure 3.

Transport delivery efficiency  $D$  as function of turnover frequency  $\nu_{\text{turn}}$  for different sets of parameters and different delivery distances  $d$ . Broken lines correspond to ideal power-stroke dependence  $D_{\text{ideal}} = L^2\nu_{\text{turn}}/d$ , to compare with.

### Figure 4.

Thermodynamic efficiency as function of loading force  $f_0$  at the end of simulations (corresponding to  $t_{\text{max}} = 2.94$  s) for different sets.

**Figure 5.**

Stalling force as function of barrier height  $U_0$  at different temperatures and fixed  $\nu_{\text{turn}} = 85$  Hz. Numerical results are compared with an analytical fit by Eq. 9 for  $U_0 > U_m T/T_r$ .

## References

1. Nelson, P. 2004. *Biological Physics: Energy, Information, Life*. Freeman and Co., New York.
2. Luby-Phelps, K. Cytoarchitecture and physical properties of cytoplasm: volume, viscosity, diffusion, intracellular surface area. *Int. Rev. Cyt.* **192**, 189-221 (2000).
3. Kubo, R. 1966. The fluctuation-dissipation theorem, *Rep. Prog. Phys.* **29**: 255-284.
4. Odijk, T. 2000. Depletion theory of protein transport in semi-dilute polymer solutions. *Biophys. J.* **79**:2314-2321.
5. Masaro, L, and Zhu, X. X. 1999. Physical models of diffusion for polymer solutions, gels and solids. *Prog. Polym. Sci.* **24**:731-775.
6. Holyst, R. et al. 2009. Scaling form of viscosity at all length-scales in poly(ethylene glycol) solutions studied by fluorescence correlation spectroscopy and capillary electrophoresis. *Phys. Chem. Chem. Phys.* **11**:9025-9032.
7. Goychuk, I. 2012. Fractional time random walk subdiffusion and anomalous transport with finite mean residence times: faster, not slower. *Phys. Rev. E.* **86**: 021113.
8. Guigas, G., Kalla, C. & Weiss, M. 2007. Probing the nanoscale viscoelasticity of intracellular fluids in living cells. *Biophys. J.* **93**: 316-323.
9. Amblard, F. et al. 1996. Subdiffusion and anomalous local viscoelasticity in actin networks, *Phys. Rev. Lett.* **77**: 4470-4473.
10. Saxton, M. J., and Jacobson, K. 1997. Single-particle tracking: applications to membrane dynamics. *Annu. Rev. Biophys. Biomol. Struct.* **26**: 373-399.
11. Qian, H. 2000. Single-particle tracking: Brownian dynamics of viscoelastic materials. *Biophys. J.* **79**: 137-143.
12. Yamada, S., Wirtz, D., and Kuo, S. C. 2000. Mechanics of living cells measured by laser tracking microrheology. *Biophys. J.* **78**:1736-1747.
13. Caspi, A., Granek, R., and Elbaum, M. 2002. Diffusion and directed motion in cellular transport. *Phys. Rev. E* **66**: 011916.

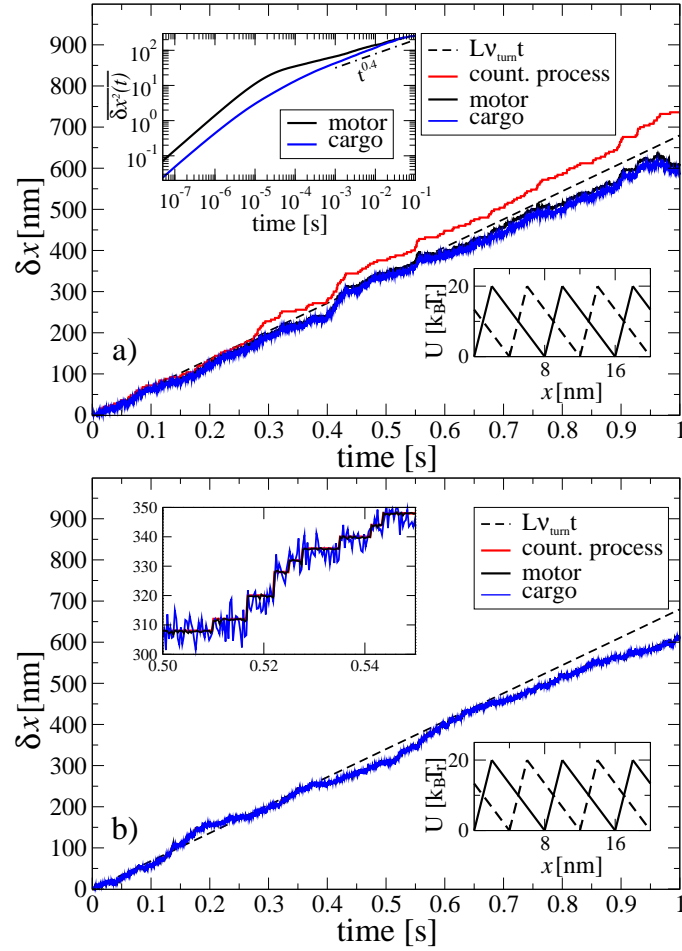


Figure 1:

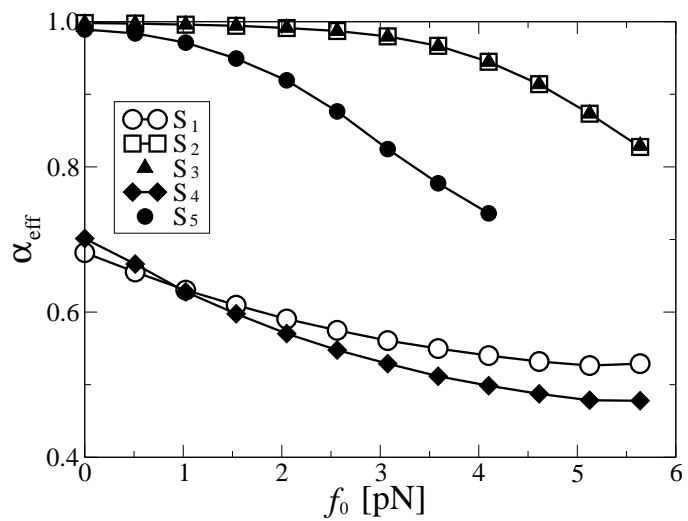


Figure 2:

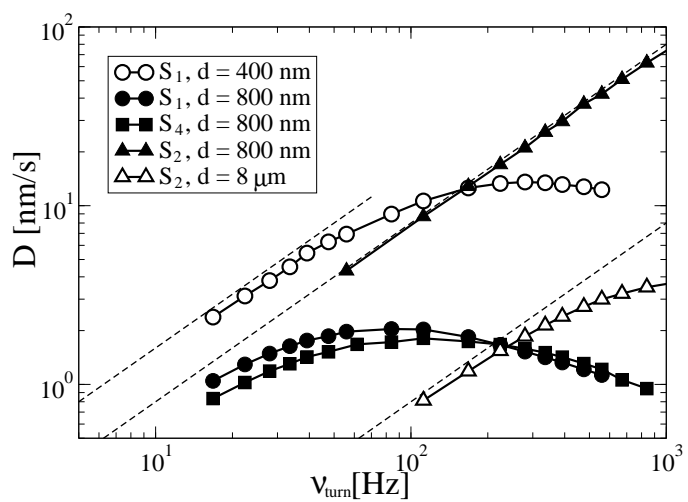


Figure 3:

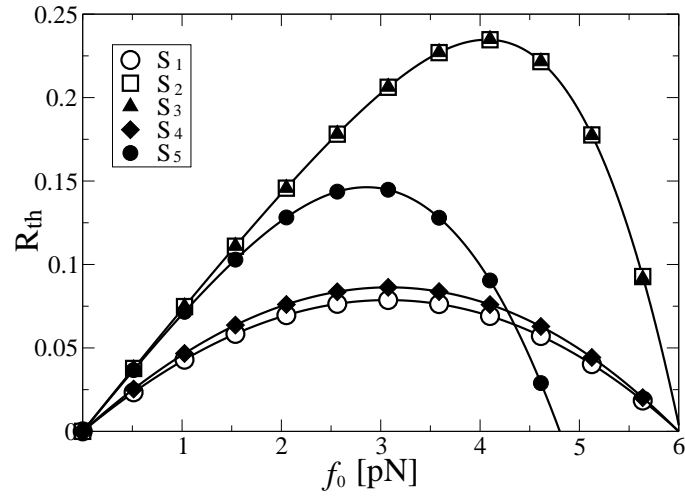


Figure 4:

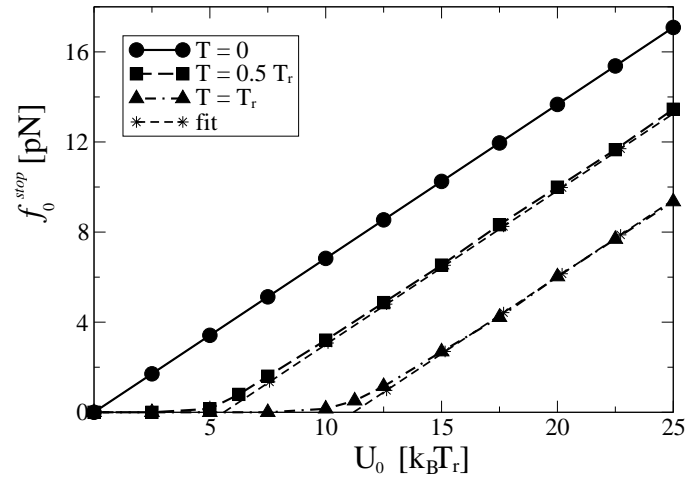


Figure 5:

14. Tolić-Nørrelykke, I. M., Munteanu, E-L., Thon, G., Oddershede, L., and Berg-Sørensen, K. 2004. Anomalous diffusion in living yeast cells, *Phys. Rev. Lett.* 93: 078102.
15. Golding, I., and Cox, E. C. 2006. Physical nature of bacterial cytoplasm. *Phys. Rev. Lett.* 96: 098102.
16. Szymanski, J., and Weiss M. 2009. Elucidating the origin of anomalous diffusion in crowded fluids. *Phys. Rev. Lett.* 103: 038102 (2009).
17. Robert, D., Nguyen, Th.-H., Gallet, F., and Wilhelm, C. 2010. In vivo determination of fluctuating forces during endosome trafficking using a combination of active and passive microrheology. *PLoS ONE* 4: e10046.
18. Bruno, L., Salierno, M., Wetzler, D. E., Desposito, M. A., Levi, V. 2011. Mechanical properties of organelles driven by microtubuli-dependent molecular motors in living cells. *PLoS ONE* 6: e18332.
19. Jeon, J. H., Tejedor, V., Burov, S., Barkai, E., Selhuber-Unkel, C., Berg-Sørensen, K., Oddershede, L. & Metzler, R. 2011. In vivo anomalous diffusion and weak ergodicity breaking of lipid granules, *Phys. Rev. Lett.* 106: 048103.
20. Jeon, J. H., Leijnse, N., Oddershede, L. B., Metzler, R. 2013. Anomalous diffusion and power-law relaxation of the time averaged mean squared displacement in worm-like micellar solutions. *New J. Phys.* 15: 045011.
21. Barkai, E., Garini, Y., and Metzler, R. 2012. Strange kinetics of single molecules in living cells. *Phys. Today* 65(8): 29-35 (2012).
22. Tabei, S. M. A., Burov, S., Kim, H. Y., Kuznetsov, A., Huynh, T., Jureller, J., Philipson, L. H., Dinner, A. R., and Scherer, N. F. 2013. Intracellular transport of insulin granules is a subordinated random walk. *Proc. Natl. Acad. Sci. USA* 110: 4911-4916.
23. Höfling, F., Franosch, T. 2013. Anomalous transport in the crowded world of biological cells. *Rep. Progr. Phys.* 76: 046602.
24. Taylor, M. A., Janousek, J., Daria, V., Knittel, J., Hage, B., Bachor, H.-A., and Bowen, W. P. 2013. Biological measurement beyond the quantum limit. *Nature Photonics* 7: 229-233.
25. Weiss, M. 2013. Single-particle tracking data reveal anticorrelated fractional Brownian motion in crowded fluids. *Phys. Rev. E* 88: 010101 (R).

26. Mandelbrot, B.B. and van Ness, J. W. 1968. Fractional Brownian motions, fractional noises and applications, *SIAM Review* 10: 422-437.
27. Goychuk, I. 2009. Viscoelastic subdiffusion: from anomalous to normal. *Phys. Rev. E* 80: 046125.
28. Wang, K. G., Tokuyama, M. Nonequilibrium statistical description of anomalous diffusion. 1999. *Physica A* 265:341-351.
29. Goychuk, I., and Hänggi, P. 2007. Anomalous escape governed by thermal  $1/f$  noise. *Phys. Rev. Lett.* 99: 200601.
30. Zwanzig, R. 1973. Nonlinear generalized Langevin equations, *J. Stat. Phys.* 9: 215-220.
31. Goychuk, I. 2012. Viscoelastic subdiffusion: Generalized Langevin Equation approach. *Adv. Chem. Phys.* 150: 187-253.
32. Zwanzig, R. 2001. Nonequilibrium statistical mechanics. Oxford University Press, Oxford.
33. Kubo, R., Toda, M., and Hashitsume, M. 1991. Nonequilibrium statistical mechanics, 2nd ed. Springer, Berlin.
34. Ellis, R. J., and Minton, A.P. 2003. Cell biology: join the crowd. *Nature* 425: 27-28.
35. McGuffee, S. R., and Elcock, A. H. 2010. Diffusion, crowding & protein stability in a dynamic molecular model of the bacterial cytoplasm. *PLoS Comput. Biol.* 6: e1000694.
36. Hirokawa, N., and Takemura, R. 2005. Molecular motors and mechanisms of directional transport in neurons. *Nature Reviews* 6: 201-214.
37. Jones, A. T., Gumbleton, M., and Duncan R.. Understanding endocytic pathways and intracellular trafficking: a prerequisite for effective design of advanced drug delivery systems. *Adv. Drug Deliv. Rev.* 55: 1353-1357.
38. Chauwin, J.-F., Ajdari, A., Prost, J. 1994. Force-free motion in asymmetric structures: a mechanism without diffusive steps. *Europhys. Lett.* 27: 421-426.
39. Jülicher, F., Ajdari, A., Prost, J. 1997. Modeling molecular motors. *Rev. Mod. Phys.* 69: 1269-1282.

40. Jülicher, F. Force and motion generation of molecular motors: A generic description. in: Müller, S. C., Parisi J., Zimmermann, W. (eds.). 1999. Transport and Structure: Their Competitive Roles in Biophysics and Chemistry. Springer, Berlin. *Lect. Not. Phys.* 532: 46-74.
41. Astumian, R. D. 1997. Thermodynamics and kinetics of a Brownian motor. *Science* 276: 917-922.
42. Astumian, R.D., Bier, M. 1996. Mechanochemical coupling of the motion of molecular motors to ATP hydrolysis. *Biophys. J.* 70: 637-653.
43. Fisher, M. E., and Kolomeisky, A. B. 2001. Simple mechanochemistry describes the dynamics of kinesin molecules. *Proc. Natl. Acad. Sci. USA* 98: 7748-7753.
44. Perez-Carrasco, R. & Sancho, J. M., Theoretical analysis of the F<sub>1</sub>-ATPase experimental data. *Biophys. J.* **98**, 2591-2600 (2010).
45. Goychuk, I. 2010. Subdiffusive Brownian ratchets rocked by a periodic force. *Chem. Phys.* 375: 450–457.
46. Goychuk, I., and Kharchenko, V. 2012. Fractional Brownian motors and Stochastic Resonance. *Phys. Rev. E* 85: 051131.
47. Kharchenko, V., and Goychuk, I. 2012. Flashing subdiffusive ratchets in viscoelastic media. *New J. Phys.* 14: 043042(2012).
48. Goychuk, I., and Kharchenko, V. 2013. Rocking subdiffusive ratchets: origin, optimization and efficiency. *Math. Model. Nat. Phenom.* 8: 144-158.
49. Kharchenko, V. & Goychuk, I. 2013. Subdiffusive rocking ratchets in viscoelastic media: Transport optimization and thermodynamic efficiency in overdamped regime. *Phys. Rev. E* 87: 052119.
50. Reimann, P. 2002. Brownian motors: noisy transport far from equilibrium. *Phys. Rep.* 361: 57-265.
51. Makhnovskii, Yu. A., Rozenbaum, V. M., Yang, D.-Y., Lin, S. H., Tsong, T. Y. 2004. Flashing ratchet model with high efficiency. *Phys. Rev. E* 69: 021102 (2004).
52. Goychuk, I., Kharchenko, V., Metzler, R. 2013. Coexistence and efficiency of normal and anomalous transport by molecular motors in living cells. arXiv:1309.6724 [physics.bio-ph].

53. Zeldovich K. B., Joanny, J.-F., and Prost, J. 2005. Motor proteins transporting cargos. *Eur. Phys. J. E* 17: 155-163.
54. Kojima, H., Muto, E., Higuchi, H., and Yanagida, T. 1997. Mechanics of single kinesin molecules measured by optical trapping nanometry. *Biophys. J.* 73: 2012-2022.
55. Mason, T. G., Weitz, D. A. 1995. Optical measurements of frequency-dependent linear viscoelastic moduli of complex fluids. *Phys. Rev. Lett.* 74: 1250-1253.
56. Waigh, T. A. 2005. Microrheology of complex fluids. *Rep. Prog. Phys.* 68: 685-742.
57. Jones, R. A. L. 2009. Soft condensed matter. Oxford University Press, Oxford.
58. Gemant, A. 1936. A method of analyzing experimental results obtained from elasto-viscous bodies. *Physics* 7: 311-317.
59. Maxwell, J. C. 1867. On the dynamical theory of gases. *Phil. Trans. R. Soc. Lond.* 157: 49-88.
60. Weiss, U. 1999. Quantum dissipative systems, 2nd. ed. World Scientific, Singapore.
61. Bruno, L., Levi, V., Brunstein, M., and Desposito, M. A. 2009. Transition to superdiffusive behavior in intracellular actin-based transport mediated by molecular motors. *Phys. Rev. E* 80: 011912.
62. Palmer, R. G., Stein, D. L., E. Abrahams, E., and Anderson, P. W. 1984. Models of hierarchically constrained dynamics for glassy relaxation, *Phys. Rev. Lett.* 53: 958-961.
63. Sekimoto, K. 1997. Kinetic characterization of heat bath and the energetics of thermal ratchet models. *J. Phys. Soc. Jpn.* 66: 1234-1237.
64. Derenyi, I., Bier, M., and Astumian, R. D.. 1999. Generalized efficiency and its application to microscopic engines. *Phys. Rev. Lett.* 83: 903-906.
65. Suzuki D., and Munakata, T. 2003. Rectification efficiency of a Brownian motor. *Phys. Rev. E* 68: 021906.
66. Wang H, and Oster, G. 2002. The Stokes efficiency for molecular motors and its applications. *Europhys. Lett.* 57: 134-140.

67. Wyman, J. 1975. The turning wheel: a study in steady states. *Proc. Nat. Acad. Sci. USA* 72: 3983-3987.
68. Gard, T. C. 1998. Introduction to Stochastic Differential Equations. Dekker, New York.

#### **Acknowledgments**

Support of this research by the German Research Foundation, Grants GO 2052/1-1 and GO 2052/1-2, as well as funding from the Academy of Finland (FiDiPro scheme) are gratefully acknowledged.